Materials Research Proceedings **27** (2023) 42-49 https://doi.org/10.21741/9781644902455-6

Experimental nondestructive detection on grout defects in a prefabricated concrete frame

Xuan Zhang[1,2,a*], Songtao Xue[1,3,b]

[1]Department of Architecture, Tohoku Institute of Technology, Sendai, Japan

[2]College of Engineering and Architecture, Shandong University of Science and Technology, Qingdao, China

[3]Department of Disaster Mitigation for Structures, Tongji University, Shanghai, China

[a]zhangxuan12341234@163.com, [b]xuest@tohtech.ac.jp

Keywords: Nondestructive Detection, Grout Defects, Prefabricated Concrete Frame, Wavelet Packet Analysis

Abstract. Researches on grout defects detection in prefabricated structures with rebars connected by sleeves are few at present. This study presents a nondestructive grout defects detection method based on wavelet packet analysis. An experiment is carried out on a prefabricated concrete frame with external sinusoidal excitation applied. Furthermore, structural acceleration responses are collected, and defects detection index the percentage of energy transfer (*PET*) is proposed based on wavelet packet analysis to identify the grout defects degree in sleeves and reasonable results are obtained.

Introduction

Prefabricated structures are constructed widely with advantages of fewer labors, lesser environmental pollution and better quality compared with cast-in-situ structures [1,2]. The joint connection methods in prefabricated structures mainly include the grout sleeve, the grout anchor and the machinery [3], in which grout sleeve connection is the most widely adopted in China. However, it is noticed that the grout defects in end sleeve caused by the leakage of slurry, the grout defects in middle sleeve caused by incompletely discharging air, or the eccentric defect of the steel rebars usually exist in in practical engineering structures that will affect the structural safety [4]. Therefore, several researchers carried out studies on detect grout defects with different methods.

The X-ray technology was used by Zhang et al. to test grouting compactness of sleeves in reinforced concrete shear walls, and results indicated that portable X-ray could clearly determine the shape of sleeves, the shape and lapping of steel bars, grouted area and hollow area [5]. Based on propagation paths of ultrasonic wave, ultrasonic wave amplitude was analyzed by Nie et al. to detect the density of grout in steel sleeves [6]. Liu carried out a series of experiments on grout sleeve specimens with different types and different grouting compactness based on impact-echo method, and results showed that the method was feasible to detect the grouting compactness of grout sleeve to some extent, but further research should be explored to improve the accuracy [7]. A hole-drilling method combined with endoscopy was proposed by Li and the quantitative assessment of the grouting plumpness of sleeve was realized [8].

It is noticed that the existing methods for grout defects identification have limits of expensive testing equipment, complex operation, or destructive detection. Accordingly, this paper proposes a nondestructive method based on dynamic excitation and wavelet packet analysis for grout defects identification in sleeves of a prefabricated frame. The experiment is conducted on a prefabricated concrete frame with column rebars connected by grout sleeves. By analyzing the structural acceleration responses based on wavelet packet, defects detection index the percentage of energy transfer (*PET*) is proposed to identify the grout defects in sleeves and good results are obtained.

Theory

Energy Spectrum Vector. Structural dynamic responses (e.g., the natural frequency, stiffness and acceleration) are generated once a structure is exerted external excitation. It is noticed that the response signals of a destructive structure are different from a nondestructive structure, resulting in the signal frequency components are redistributed. Wavelet packet decomposition is a refined signal analysis method that can improve the time-frequency resolution by decomposing the low-frequency signal and high-frequency signal simultaneously [9]. Through extracting the energy value of each frequency band, the characteristic vectors are formed to identify structural defects.

(1) x represents the structural response signal, which is decomposed by wavelet packet into j layers.

(2) E_j^i represents the energy of i-th node in the j-th layer calculated according to Eq. 1.

$$E_j^i = \sum_{i=1}^{2^j} \left| x_j^{i,k} \right|^2 . \tag{1}$$

where $x_j^{i,k}(k=1,2,\ldots, n)$ represents the amplitude of discrete point in reconstructed signal; n represents the number of discrete points.

(3) Energy spectrum vector is constructed, as shown in Eq. 2.

$$T = \left\{ E_j^1, E_j^2, \ldots E_j^{2^j} \right\}. \tag{2}$$

Wavelet Function. The wavelet function has characteristics of orthogonality, local property in time domain and nondestructive property in signal reconstruction [10]. Accordingly, *sym*8 is chosen in this paper, and the corresponding wavelet function and scaling function are seen in Fig. 1.

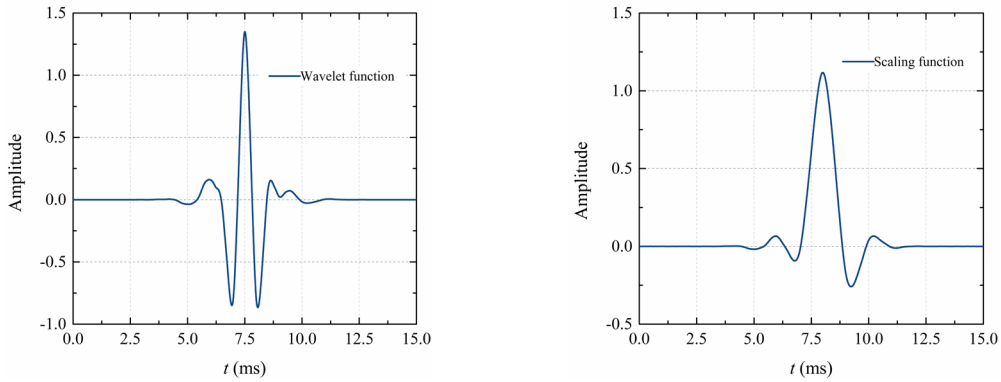

(a) Wavelet function *(b) Scaling function*

Figure 1. Sym8 function

Decomposed Level. As the signal decomposed layer increases, structural defects detection becomes more sensitive, but it cost longer computing time. Therefore, cost function is defined in Eq. 3 to select appropriate decomposition layer to construct a reasonable energy spectrum. The reasonable decomposition level meets the condition that the smaller $S_L(E_j)$ and shorter computing time.

$$S_L(E_j) = \sum_{i=1}^{2^j} \left| E_j^i \right|^p, \quad 1 \le p \le 2 . \tag{3}$$

Defects Detection Index. Based on wavelet packet decomposition, signal energy in each frequency band is extracted and combined to obtain the defect detection index. Li and Sun [11] have shown that the changes of energy in each frequency band can effectively identify the defects in

Materials Research Proceedings **27** (2023) 42-49 https://doi.org/10.21741/9781644902455-6

frame structure. Therefore, a defects detection index percentage of energy transfer (*PET*) is proposed in Eq. 4.

$$PET = \frac{1}{2} \times \sum_{i=1}^{2^j} \left| \frac{E_{j,d}^i}{\sum_{k=1}^{2^j} E_{j,d}^i} - \frac{E_{j,n}^i}{\sum_{k=1}^{2^j} E_{j,n}^i} \right| \times 100 \,. \tag{4}$$

where $E_{j,d}^i$ represents the energy of i-th node in the j-th layer in destructive structure, $E_{j,n}^i$ represents the energy of i-th node in the j-th layer in nondestructive structure.

Experimental Study

Experimental Model. As presented in Fig. 2, the experimental structure is a 1/2-scaled prefabricated concrete frame with two floors, in which column rebars are connected by grouted sleeves. The concrete compressive strength is 25 MPa, and the yield strength of longitudinal reinforcement and stirrup is 400 MPa.

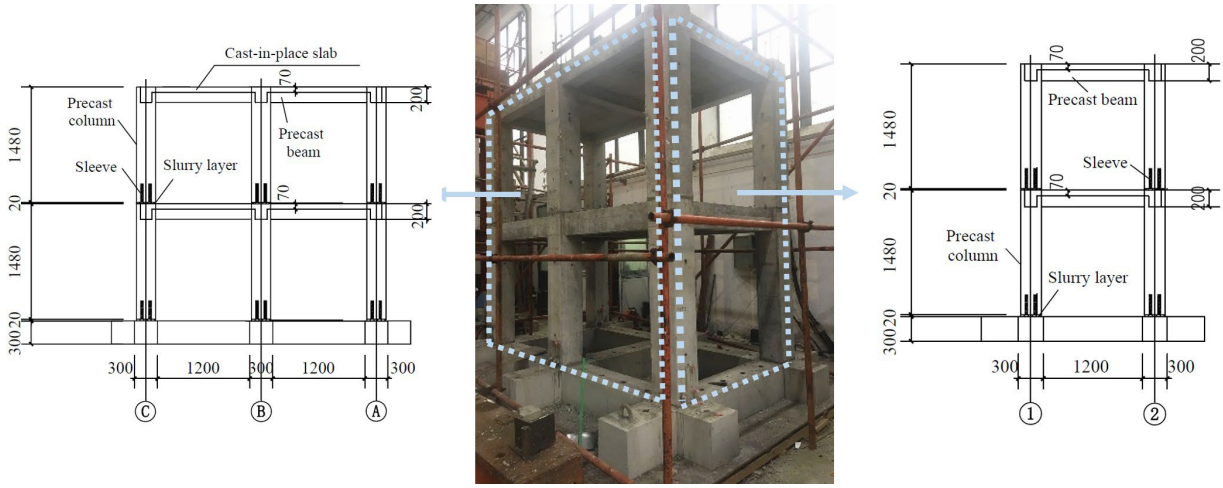

Figure 2. Experimental model

Layout of Defects, Excitation and Monitoring Points. Several sleeves in the first floor are not grouted compactly due to constructional deviation. Artificial initial sleeve grout defects are in the second floor, which is implemented by not grouting at all.

Fig. 3 presents the layout of defects, excitation points (recorded as EP) and monitoring points (recorded as MP) in the second floor. The hollow circle in column represents the sleeve is not grouted at all, and the black circle represents the sleeve is intact grouted. There are six designed cases totally, and in every case one column is destructive while the other one is nondestructive. To be specific, in columns No.2, No.4, and No.6, there are 3, 1, 2 hollow sleeves respectively, and all sleeves are intact grouted in columns No.1, No.3, and No.5. Comparing the cases 1-3 in structural longitude direction, defects degree in case 1 is the most severe, followed by case 3, and the least is condition 2. Comparing the cases 4-6 in structural transverse direction, defects in case 5 is the most severe, followed by case 6, and the least is condition 4. Corresponding the six cases, there are six EPs totally, which are in the middle of the beam upper surface.

The monitoring points are on the column facade along the height. Taking case 5 as an example, there are both four MPs in the two columns, where MP1-MP4 located in nondestructive column No.5, MP5-MP8 located in destructive column No.2. MP1 and MP5 form the pair-wise monitoring points, recorded as MP1_5. Similarly, pair-wise monitoring points MP2_6, MP3_7 and MP4_8

are obtained. In each case, the distance of MP1_5, MP2_6, MP3_7 and MP4_8 from the column bottom are 20 mm, 320 mm, 640 mm, and 960 mm, respectively.

Experimental Instruments. In the experiment, external sinusoidal excitation with max amplitude 200 N is applied using the vibration exciter, signal source, and power amplifier. Acceleration sensors are patched on the monitoring points, at the same time, the data acquisition system of Beijing Oriental vibration and noise technology research institute is used to collect acceleration responses with acquisition frequency 1024 Hz. Taking case 5 as an example, the arrangement of experimental instruments is showed in Fig. 4.

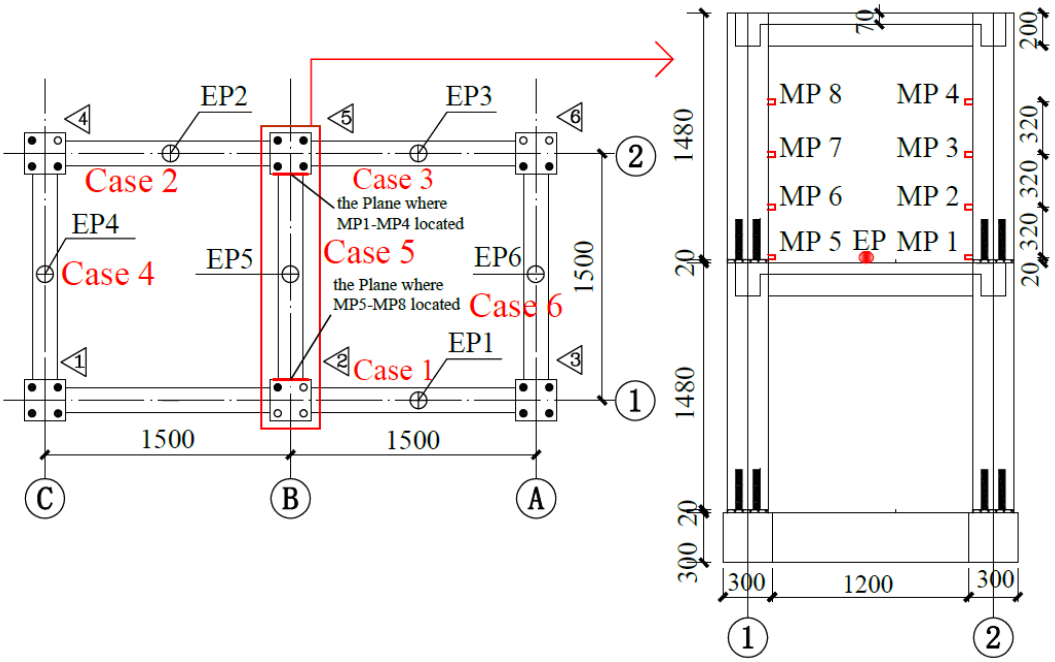

Figure 3. Layout of defects, excitation and monitoring points

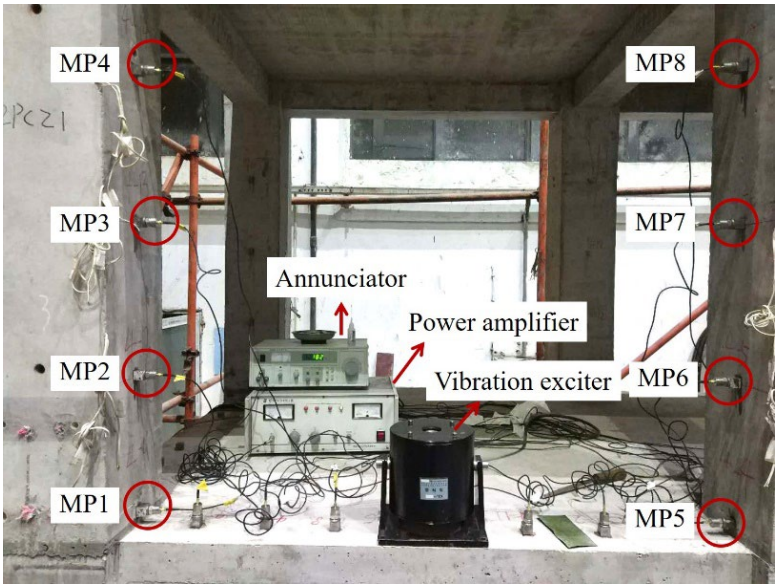

Figure 4. Arrangement of the experimental instrument in case 5

Results and Analysis

Acceleration Responses. The variational trend of acceleration responses of all monitoring points in cases 1–6 are similar. Taking case 4 as an example, Fig. 5 shows acceleration curves of MP1-MP8 (all are representative excerpts), in which the blue curves are obtained by MP1-MP4 located

Materials Research Proceedings **27** (2023) 42-49 https://doi.org/10.21741/9781644902455-6

in nondestructive column, and the red curves are obtained by MP5-MP8 located in destructive column. It is observed that the amplitudes of pair-wise points MP1_5, MP2_6, MP3_7, and MP4_8 are different, indicating the grout sleeve defects have influenced structural acceleration responses.

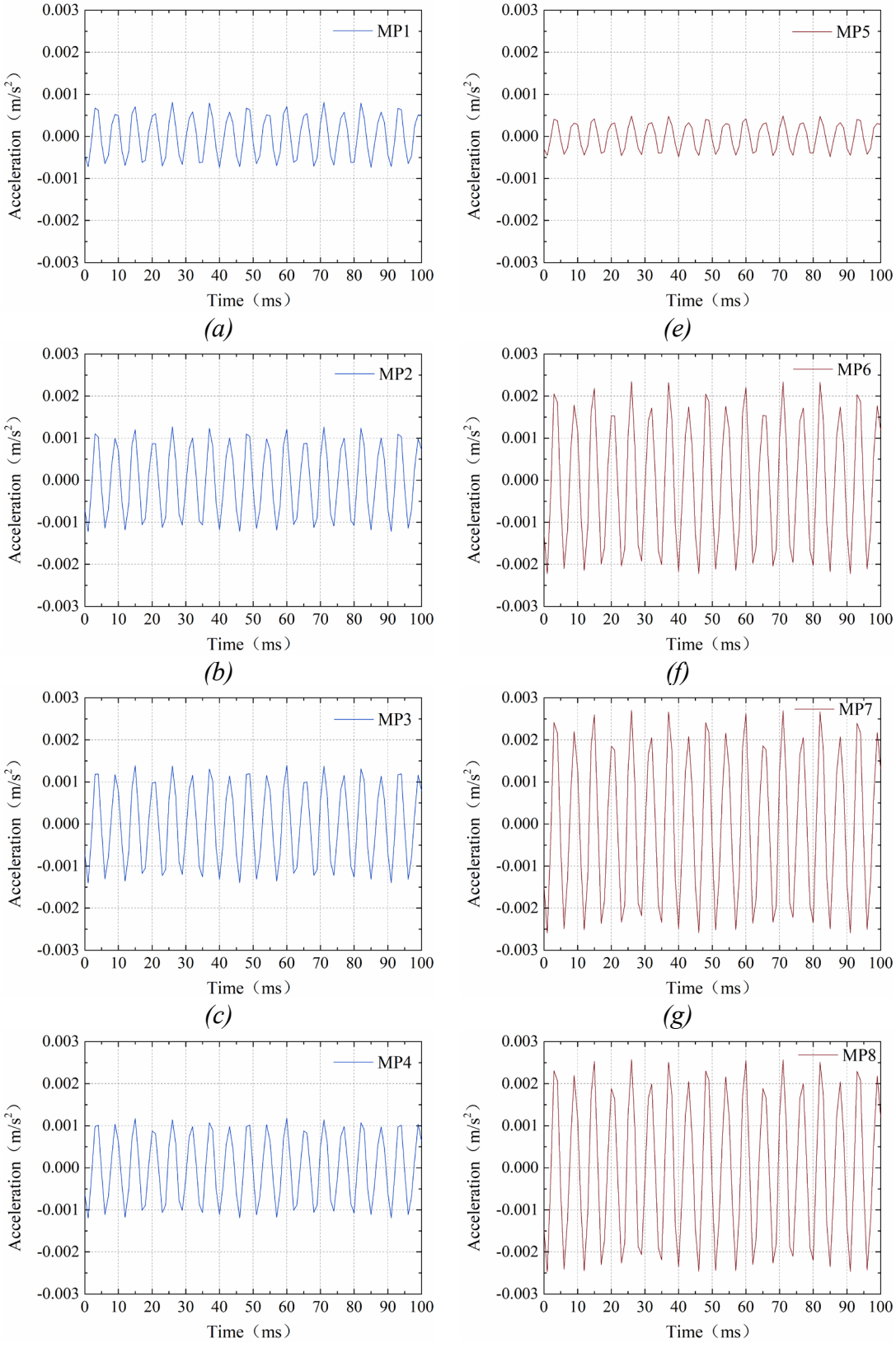

Figure 5. Acceleration responses of case 4

Decomposed Level. Taking the acceleration responses of MP6 in cases 1 and 6 as examples, cost function $S_L(E_j)$ under decomposed levels 9-15 are calculated according to Eq. 3, as shown in Table 1. It is seen that with decomposed level increases, $S_L(E_j)$ becomes smaller, while longer computing time cost. It is reasonable to adopt decomposed level 13 with relatively smaller cost function and shorter computing time.

Table 1. Cost function $S_L(E_j)$ and computing time

Decomposed level		9	10	11	12	13	14	15
Case 1	$S_L(E_j)$ [$\times 10^{-3}$]	3.10	3.10	3.00	2.80	2.10	1.90	1.20
	Time[s]	1.27	2.91	7.20	19.52	55.25	281.28	1073.49
Case 6	$S_L(E_j)$ [$\times 10^{-3}$]	12.2	12.2	12.1	11.9	11.7	11.0	9.90
	Time[s]	1.27	3.19	7.11	19.36	55.17	278.89	1060.98

Defects Detection Index. Defects detection index *PET* is calculated according to Eq. 4 based on the acceleration responses of pair-wise MPs, and the indexes of MP1_5, MP2_6 MP3_7 MP4_8 are recorded as *PET1*, *PET2*, *PET3*, and *PET4* respectively.

Table 2 shows the *PET* indexes of every case. As cases 1-3 and 4-6 are separately located in the structural longitude and transverse direction, cases 1-3 and 4-6 are analyzed individually.

Table 2. PET values in cases 1-6

PET [%]	Case 1	Case 2	Case 3	Case 4	Case 5	Case 6
*PET*1	54.17	31.04	42.96	0.88	15.40	2.411
PET2	20.31	9.07	20.43	0.79	12.59	1.79
*PET*3	20.16	6.03	20.15	1.19	11.86	4.05
*PET*4	17.25	13.48	24.99	1.24	10.68	4.54

Firstly, cases 1-3 are analyzed. Compared *PET1* in every case, the index 54.17 in case 1 is biggest, followed by 42.96 in case 3, and the smallest is 31.04 in case 2. The same law is founded in *PET3*. At the same time, it is noticed that grout defects degree in case 1 is the most severe, followed by case 3, and the least is case 2. That is to say, *PET1* and *PET 3* are increased with grout defects degree except for *PET2* and *PET4*. In addition, cases 4-6 are analyzed. *PET1* values in case 4, 5, 6 are respectively 0.88, 15.40, 2.411, and grout defects in case 5 is the most severe, followed by case 6, and the least is case 4. Therefore, *PET1* value becomes larger with defects degree increases, and the same law also exist in *PET2*, *PET3*, and *PET4*.

In general, defect detection index *PET* shows a good sensitivity to grout defects except for *PET2* and *PET4* in cases 1-3. Furthermore, total defects detection index *PETs* is chosen, as presented in Eq. 5.

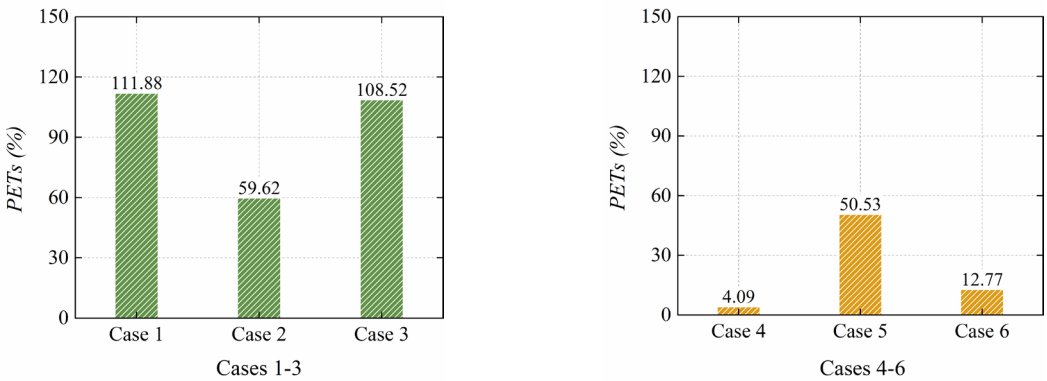

(a) PETs in cases 1-3 *(b) PETs in cases 4-6*

Figure 6. PETs values in cases 1-6

$$PETs = \sum_{i=1}^{4} PETi \,. \tag{5}$$

Fig. 6 shows *PETs* in cases 1-3 and 4-6, it is seen that total detection index *PETs* is positively correlated with column grout defects degree, showing a good grout detection result in every case. At the same time, it is noted that parts of sleeve grout in the first floor are destructive, which proves that the proposed detective method is not influenced by the defects of another floor obviously.

Conclusion

Experimental nondestructive detection on grout defects in a prefabricated concrete frame with wavelet packet analysis is carried out in this paper, and the main conclusions are drawn as following:

(1) The acceleration responses of the pair-wise monitoring points, respectively located in destructive column and nondestructive column, are different in amplitudes.

(2) Defects detection index *PET* cannot well identify the grout defects in individual cases, while total defects detection index *PETs* shows a good grout detection result having positively correlation with column grout defects degree in all cases.

(3) The effect of proposed grout defect detective method is not influenced by the defects of another floor obviously.

Acknowledgments

This research was funded by the “Japan Society for the Promotion of Science, grant number P21790”, the “Japan Society for the Promotion of Science, grant number 18K04438”, the “Tohoku Institute of Technology Research Grant”, and the “Introduction and education plan for young innovative talents in colleges and universities of Shandong Province (Marine Civil Engineering Materials and Structure Innovation Research Team). The financial support is gratefully acknowledged.

References

[1] Han J Q. Study on seismic performance of prefabricated-reinforce concrete junction. Chemical Engineering Transactions, 2016, 51, pp.1105-1110.

[2] Yin W Y, Xia S, Zhang X, et al. Precast concrete frame structure. Applied Mechanics and Materials, 2012, 256-259, pp.934-937. https://doi.org/10.4028/www.scientific.net/AMM.256-259.934

[3] Ministry of Housing and Urban-Rural Development of the People’s Republic of China. Technical specification for precast concrete structures, Beijing, 2014.

[4] Zheng Q L, Wang N, Tao L, et al. Experimental study on effects of grout defects on the connection behaviors of grout sleeve splicing for reinforcing bars. Building Science, 2017, 33(5), pp.61-68.

[5] Zhang F W, Li X M, Gao R D, et al. Study on detection of grouting compactness of grout sleeve by portable X-ray technology. Construction Technology, 2017, 46(17), pp.6-9+61.

[6] Nie D L, Jia L G, Du M K, et al. Experimental study on detecting density of grouting materials for steel sleeves by using ultrasonic wave. Concrete, 2014, (9), pp.120-123.

[7] Liu H, Li X M, and Xu Q F. Test on detection of grouting compactness of grout sleeve by impact-echo method. Nondestructive Testing, 2017, 39(4), pp.12-16.

[8] Li X M, Gao R D, Xu Q F, et al. Experimental study on testing grouting plumpness of sleeve by hole-drilling method combined with endoscopy. Construction Technology, 2019, 48(9), pp.6-16.

[9] He H X,p Chen K and Yan W M. Structural seismic damage assessment based on wavelet packet transformation and time-varying frequencies. Journal of Vibration and Shock, 2016, 35(7), pp.23-30.

[10] Yang J G. Wavelet Analysis and its engineering applications. 1th ed. Beijing: China Machine Press, 2005.

[11] Li H N, Sun H M. Damage diagnosis of framework structure based on wavelet packet analysis and neural network. Earthquake Engineering and Engineering Vibration, 2003, 23(5), pp.141-148.